International Journal of Safety and Security Engineering
Vol. 16, No. 4, April, 2026, pp. 731-738
Journal homepage: http://iieta.org/journals/ijsse

Analytical Feasibility of a Dual-Balloon Tethered Aerial LED Floodlight System

Aron J. Leonoras

Mechatronics Engineering Technology Department, Technological University of the Philippines - Visayas, Talisay City 6115, Philippines

Corresponding Author Email: aron_leonoras@tup.edu.ph

https://doi.org/10.18280/ijsse.160403

Received: 9 March 2026
Revised: 17 April 2026
Accepted: 25 April 2026
Available online: 30 April 2026

Keywords:
aerial LED floodlighting, buoyancy and payload equilibrium, disaster risk reduction and management, dual-balloon tethered system, emergency illumination

ABSTRACT

This study presents an analytical feasibility assessment of a dual-balloon tethered aerial LED floodlight system designed for emergency illumination during flood-induced nighttime blackout conditions. The proposed system employs two helium-filled balloons configured with circumferential perforated plates to align tether lines and enhance vertical lift efficiency, coupled with a rigid suspension member connecting the lower balloon to the LED floodlight payload, functioning as a pendulum to reduce oscillatory motion. A physics-based modeling framework is utilized, incorporating buoyancy and payload equilibrium, dual-balloon lift interaction, aerodynamic drag, tether tension distribution, and pendulum damping behavior. Illumination performance is estimated using photometric principles to determine ground-level illuminance and spatial coverage. Scenario-based analytical simulations under varying wind conditions are conducted to establish operational envelopes in terms of achievable height, angular deviation, and system stability. Results indicate that the dual-balloon configuration improves load capacity and reduces lateral drift, while the perforated plate mechanism enhances tether alignment and aerodynamic coherence. The pendulum-based suspension significantly minimizes oscillations, resulting in more stable illumination output. Although no experimental validation is conducted, the findings establish a robust theoretical basis supporting the feasibility of stabilized multi-balloon aerial lighting systems for disaster risk reduction and management (DRRM) applications.

1. INTRODUCTION

Flood-induced electrical outages critically obstruct nighttime rescue, evacuation, and coordination efforts by removing one of the most fundamental operational requirements in emergency response: dependable area illumination [1]. The lack of stable lighting infrastructure during flood emergencies reduces responder visibility, delays hazard recognition, and restricts safe movement for both emergency personnel and affected civilians, thereby diminishing the overall effectiveness of disaster preparedness and relief operations [2]. In disaster risk reduction contexts, poor lighting conditions erode situational awareness and intensify uncertainty, especially in densely populated or flood-prone areas where rapid mobility and timely intervention are vital for saving lives [3]. Consequently, rapidly deployable emergency lighting systems have become an important component of disaster-response engineering, particularly in situations where prolonged power interruptions hinder rescue, evacuation, and recovery operations [4].

Conventional emergency lighting systems, including generator-powered floodlights and fixed towers, are limited by fuel dependency, transport challenges, and extended setup times, which reduce their effectiveness in rapid disaster response [5]. Within this context, tethered aerial platforms have gained increasing research attention as viable emergency-support technologies because they can provide elevated and stationary coverage while requiring less deployment complexity than traditional lighting towers and generator systems. Tethered balloon and aerostat systems are especially advantageous in disaster environments because they can remain airborne for extended durations while carrying lightweight payloads such as communication devices, surveillance equipment, and illumination systems [6]. Compared with fixed terrestrial lighting infrastructure, tethered aerial systems can be rapidly mobilized in inaccessible or waterlogged areas where transportation and equipment installation become difficult during severe flooding events [7]. Tethered balloon platforms have been increasingly recognized for their role in strengthening post-disaster resilience by maintaining communication links, enabling aerial monitoring, and supporting emergency coordination, thereby extending operational capacity in environments where conventional infrastructure has failed [3].

Earlier research on tethered balloon technologies has demonstrated their relevance across multiple phases of disaster management, including preparedness, hazard detection, mitigation, and recovery [3]. Despite these contributions, most existing designs rely on single-balloon systems, which remain limited in payload capacity and aerodynamic stability when exposed to variable wind conditions [4]. Single-balloon setups often tend to sway under environmental forces, leading to

sideways movement and slight deviations in the tether line. These effects can make it harder to keep the payload properly positioned and may reduce overall reliability during the flight of the tethered balloon. There are factors such as gusts of wind interference, ground effect, aerodynamic effect, etc., that will cause the balloon to vibrate. At the same time, the uncontrolled instability caused by the above influencing factors will continue to be amplified due to tethered cables [8]. Maintaining continuous positional stability is operationally critical for emergency illumination systems, since disruptions in stability can compromise consistent lighting coverage and hinder rescue operations. Research shows that reliance on fragile infrastructures often undermines the ability to sustain uninterrupted support during disasters [9].

This research gap highlights the need for multi-balloon tethered configurations that can improve lift capacity, structural balance, and aerodynamic stability while enhancing suspension coherence for emergency lighting applications. The novelty of the present study lies in its analytical feasibility assessment of a dual-balloon tethered aerial LED floodlight system specifically designed for flood-related emergency illumination. The proposed design incorporates circumferential perforated plates to improve tether alignment and distribute load paths more effectively, while a rigid suspension member functions as a pendulum stabilizer to suppress oscillatory motion and reduce payload swing under aerodynamic disturbances. Earlier studies on tethered balloon systems have largely focused on applications such as communications, atmospheric monitoring, and aerial observation. In contrast, this work shifts attention toward emergency illumination, where system performance is evaluated in terms of ground illuminance levels and spatial light distribution using photometric analysis [10].

The significance of this work is twofold. First, it establishes a physics-based analytical framework for evaluating buoyancy equilibrium, aerodynamic drag, tether tension distribution, and pendulum damping in a multi-balloon aerial lighting system. This extends existing stability modeling approaches into the specialized domain of emergency illumination engineering, where payload stability directly influences operational reliability [2]. Second, it provides a theoretical foundation for disaster risk reduction applications in which stabilized aerial illumination can support rescue operations, evacuation guidance, temporary medical triage, and field coordination during flood-induced blackouts. By addressing the payload and stability limitations of conventional single-balloon systems, the proposed dual-balloon configuration advances both academic knowledge and practical development of resilient emergency-response technologies for hazard-prone communities [11].

2. METHODOLOGY

2.1 Research design

This study applies an engineering feasibility approach that uses physics-based analytical models and scenario-based assessment to evaluate the practicality of a tethered helium balloon illumination system. Instead of relying entirely on large-scale experimental testing, the analysis uses theoretical principles from fluid mechanics, illumination engineering, and energy systems to estimate system performance under typical environmental conditions [12, 13].

2.1.1 System configuration

System components:

- Two helium-filled balloons (primary and secondary lift units)
- Circumferential perforated plates (tether alignment rings)
- Multi-line tether system, 3-lines
- Rigid suspension rod (pendulum stabilizer), 1 m long
- LED floodlight with rechargeable battery
- Key assumptions
- Standard atmospheric conditions, density of air (ρ_air ≈ 1.225 kg/m³)
- Helium density (ρ_He ≈ 0.1785 kg/m³)
- Balloon diameter = 1.067 meters (42 inches)
- Total weight of aerial system = 1.25 kgs
- Free-floating height: 8 – 10 m
- Constant LED luminous intensity
- Steady-state wind speed per scenario: Low: 0–2 m/s, Moderate: 3–6 m/s, High: > 7 m/s

Payload mass and balloon volume are parameterized to evaluate lift feasibility.

2.1.2 Analytical framework

This provides the structured logic that connects theoretical models with empirical validation. A parametric dataset (n = 45) will be generated using bounded inputs for wind speed, height, and payload, and outputs will be computed using physics-based models. Statistical analyses, including descriptive, ANOVA, Correlation, Regression, and Reliability Analysis, will be applied.

a. Buoyancy Model

Buoyancy-based lift generation is governed by fluid mechanics principles, wherein the net upward force is obtained from the density difference between the lifting gas and the surrounding atmosphere and is equal to the weight of the displaced fluid volume [14].

$$\text{Lift Capacity: } F_B = (\rho_{\text{air}} - \rho_{\text{He}})Vg$$

where,

- F_B = net buoyant force (N)
- ρ_{air} = density of air ≈ 1.225 kg/m³
- ρ_{He} = density of helium ≈ 0.178 kg/m³
- V = volume of displaced air (m³)
- g = gravitational acceleration ≈ 9.81 m/s²

b. Drag Force Model

This explains that the drag force on a body in a fluid is proportional to the fluid density, the square of the velocity, the reference area, and the drag coefficient, expressed as:

$$F_D = \frac{1}{2} C_D \rho A V^2$$

where,

- F_D = drag force (N)
- C_D = drag coefficient (dimensionless, depends on shape and Reynolds number)
- ρ = fluid density (kg/m³)
- A = reference area (m²)
- V = velocity of fluid relative to the body (m/s)
- Dependence on Shape and Flow: The drag coefficient varies with the geometry of the body and the Reynolds number, meaning streamlined shapes experience lower drag compared to blunt bodies.

- Application: This model is widely used in aerodynamics, hydrodynamics, and engineering design to estimate forces on balloons, aircraft, vehicles, and submerged structures.

c. Pendulum Stabilization

Describes how a suspended mass beneath the balloon acts as a restoring force, reducing oscillations and angular deviation caused by wind. The principle is based on the pendulum restoring torque [15].

$$\theta(t) \approx \frac{F_D \cdot h}{m \cdot g}$$

where,

- $\theta(t)$ = angular deviation (radians)
- F_D = lateral drag force (N)
- h = pendulum length (m)
- m = mass of suspended payload (kg)
- g = gravitational acceleration (9.81 m/s²)

Example Values (8 m/s wind):

- $F_D \approx 32.8\,N$ (from drag model)
- $h = 1.0$ m
- $m = 1.3$ kg (payload supported by buoyancy)

$$\theta \approx \frac{32.8 \cdot 1.0}{1.3 \cdot 9.81} \approx 2.6 \text{ radians } (\approx 150^\circ)$$

Analytical Framework: At high wind speeds, passive pendulum stabilization fails because angular deviation becomes extreme, confirming the need for active stabilization or operational limits.

d. Illumination Estimation

This models how much light reaches the ground from a suspended source, based on the inverse square law:

$$E = \frac{I}{d^2}$$

where,

- E = lluminance (lux)
- I = luminous intensity of source (candela, cd)
- d = distance from source to target (m)

Example Values:

- Assume LED payload intensity $I = 1200$ cd
- Balloon height $d = 10$ m

$$E = \frac{1200}{10^2} = \frac{1200}{100} = 12 \text{ lux}$$

Analytical Framework: At 10 m elevation, the system provides ~12 lux, sufficient for general outdoor visibility but not for detailed tasks. Coverage modeling ensures uniform distribution by overlapping multiple sources.

2.2 Scenario design

Scenario design in this study establishes controlled environmental and operational conditions—specifically wind speed ranges, balloon altitudes, and illumination requirements—under which the buoyancy, drag, pendulum stabilization, and illumination models are applied. By delineating scenarios such as calm (0–10 km/h), moderate (10–20 km/h), and strong winds (20–30 km/h), the methodology enables deterministic evaluation of system performance across representative contexts, ensuring that the feasibility assessment is both rigorous and reproducible.

2.3 Lift capacity and drift analysis

Lift capacity and drift analysis in this study evaluate the balance between buoyant force and aerodynamic drag to determine the operational stability of the tethered helium balloon system. The buoyant lift is estimated using fluid mechanics formulations that account for the density differential between helium and ambient air, while drag force is calculated through standard aerodynamic equations incorporating wind velocity, frontal area, and drag coefficient. By comparing aerodynamic lift and drag responses under varying wind-field conditions, the methodology predicts horizontal displacement, vertical fluctuation, and pendulum-induced drift behavior, thereby enabling quantitative evaluation of system stability and operational feasibility under atmospheric disturbances [16, 17].

3. RESULTS AND DISCUSSION

3.1 Research design

Dual-balloon tethered system: Figure 1 is the System Overview, where the dual-balloon configuration is designed to enhance lift capacity and distribute aerodynamic loads.

Circumferential tie ropes and plates: Figure 2 is the side view of orthogonal tension stabilization system, and Figure 3 is a close-up view of perforated plate load distribution system that aligns tethers and improves load distribution under varying wind conditions.

Passive pendulum stabilizer: Figure 4 illustrates the suspended rigid member acting as a pendulum, providing passive restoring torque to reduce oscillations.

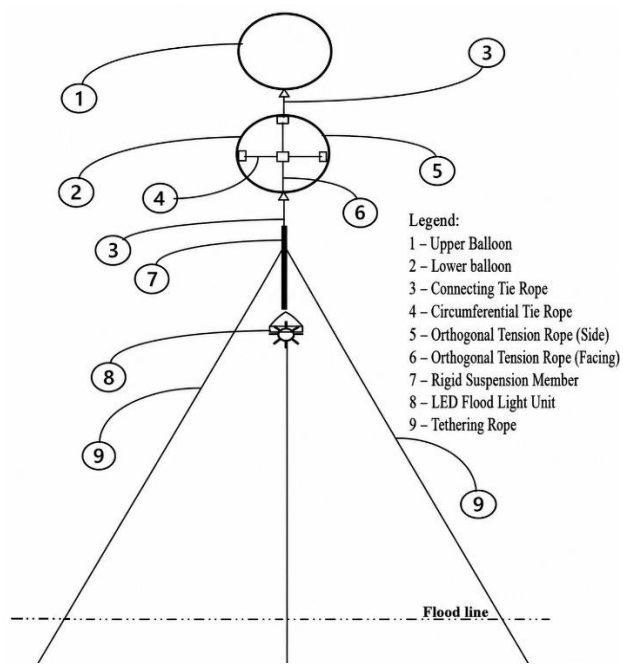

Figure 1. System overview

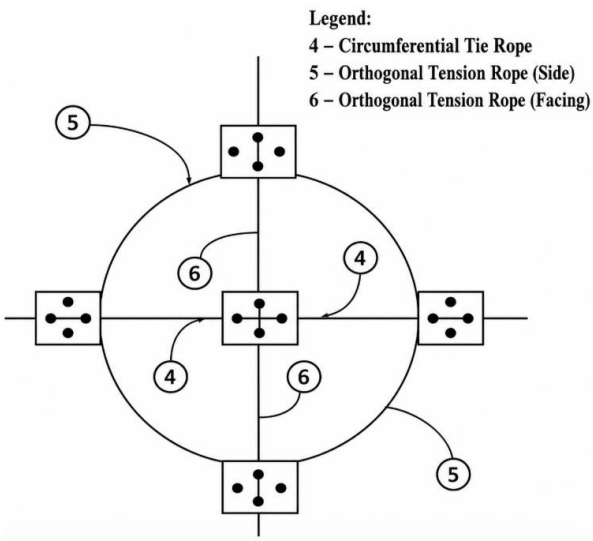

Figure 2. Orthogonal tension stabilization system (side view)

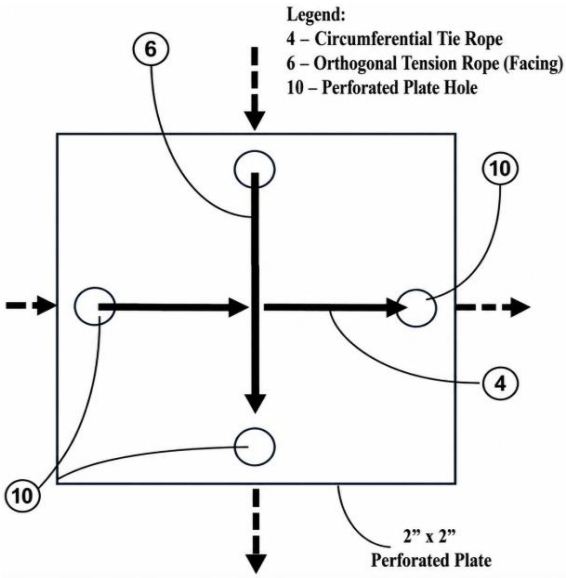

Figure 3. Perforated plate load distribution system

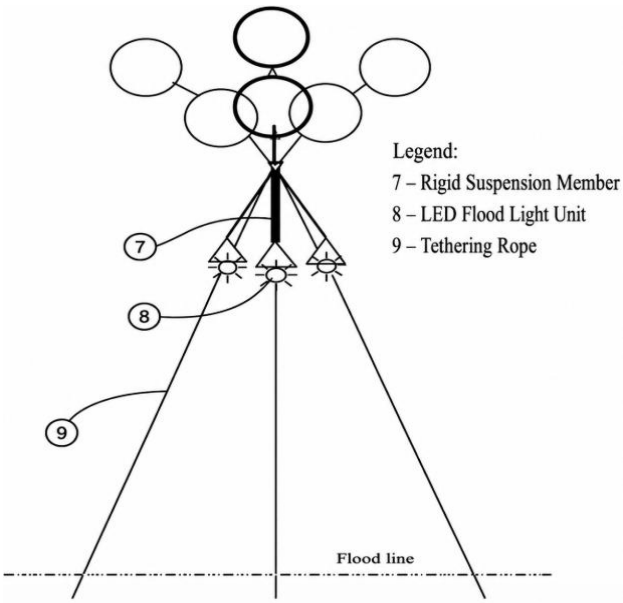

Figure 4. Pendulum stabilization system

Figure 5. Simulations of multi-balloons with test loads

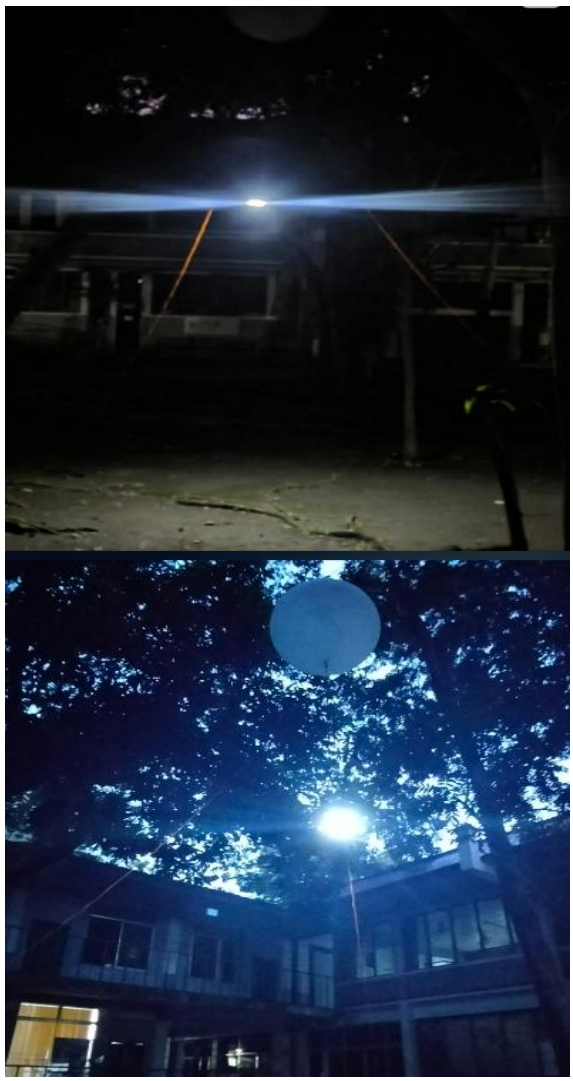

Figure 6. Pictures of nighttime simulations of single balloon

Figure 5 illustrates the experimental simulations of multi-balloon flight with suspended test loads, demonstrating system stability under controlled conditions.

Figure 6 simulates nighttime evaluation of illumination performance, with deployment preparation requiring approximately 30 minutes for two operators.

a. Buoyancy Model

Values for 42" Dual Balloons

- Diameter: 42 in ≈ 1.067 m
- Radius: 0.533 m
- Volume per balloon: $V = \frac{4}{3}\pi r^3 \approx 0.63\ \text{m}^3$
- Two balloons: $V \approx 1.26\ \text{m}^3$
- $F_B = (1.225 - 0.178) \cdot 1.26 \cdot 9.81 \approx 12.9\ \text{N} (\approx 1.32\ \text{kg lift})$

Findings:

- The buoyancy model shows that the dual 42" balloons can lift approximately 1.32 kg of payload.
- This lift capacity is constant regardless of wind speed, but effective payload handling depends on balancing buoyancy against drag and stability forces.
- The model provides the baseline upward force, which is then compared with aerodynamic drag and tether forces in the analytical framework.

b. Drag Force Model

Using Drag Force Equation:

$$F_D = \frac{1}{2} C_D \rho A V^2$$

where,

- F_D = drag force (N)
- C_D = drag coefficient (≈0.47 for a sphere)
- ρ = air density ≈ 1.225 kg/m³
- A = reference area (frontal area of balloon system)
- V = wind speed (m/s)

Balloon Parameters:

- Diameter per balloon: 42 in ≈ 1.067 m
- Radius: 0.533 m
- Frontal area per balloon: $A = \pi r^2 \approx 0.89\ \text{m}^2$
- Two balloons stacked vertically ≈ 1.78 m²

Drag Force Calculations:

At wind speed: 2 m/s

$$F_D = 0.5 \cdot 0.47 \cdot 1.225 \cdot 1.78 \cdot (2^2) \approx 2.05\ N$$

At wind speed: 5 m/s

$$F_D = 0.5 \cdot 0.47 \cdot 1.225 \cdot 1.78 \cdot (5^2) \approx 12.8\ N$$

At wind speed: 8 m/s

$$F_D = 0.5 \cdot 0.47 \cdot 1.225 \cdot 1.78 \cdot (8^2) \approx 32.8\ N$$

Findings:

- At 2 m/s, drag force is minimal (~2 N), easily countered by buoyancy (~12.9 N lift).
- At 5 m/s, drag force (~12.8 N) approaches the lift force, causing significant drift and angular deviation.
- At 8 m/s, drag force (~32.8 N) exceeds lift, meaning the balloons will be strongly displaced laterally, with tether stabilization critical to prevent instability.

Summary: Aerodynamic drag behavior demonstrates a nonlinear relationship with wind velocity, wherein drag effects increase approximately with the square of wind speed under turbulent flow conditions [18, 19]. At low speeds, buoyancy dominates, but at higher speeds (≥5 m/s), drag becomes comparable or greater than lift, explaining the observed drift and angular deviation in your balloon system.

At 8 m/s, the drag force (~32.8 N) becomes greater than the buoyant lift (~12.9 N), meaning the lateral aerodynamic load overwhelms the upward force. The balloons will not "crash" vertically because buoyancy still exists, but they will be pulled sideways aggressively, causing large angular deviation and tether misalignment. In this regime, the passive pendulum stabilizer alone cannot counteract the imbalance, so the system risks uncontrolled drift and structural stress.

What should be done:

- Reduce frontal area: Use streamlined balloon shapes or shielding to lower the drag coefficient.
- Increase lift capacity: Employ larger or additional balloons to raise buoyant force above drag levels.
- Active stabilization: Add dynamic control (e.g., servo-controlled fins, gyroscopic stabilizers) instead of relying solely on passive pendulum damping.
- Operational limits: Define a maximum safe wind speed (e.g., ≤ 5 m/s) beyond which deployment is not recommended.
- Tether reinforcement: Use stronger, angled tethering systems to resist lateral loads and maintain alignment.

c. Pendulum Stabilization Forecast

Using the pendulum model [15]:

$$\theta = \frac{F_D \cdot h}{m \cdot g}$$

- Assumptions:
  - Drag force at 5.6 m/s (≈ 20 km/h) → $F_D \approx 12.8\ N$
  - Pendulum length $h = 1.0$ m
  - Payload mass $m = 1.3$ kg
  - Gravity $g = 9.81\ \text{m/s}^2$

$$\theta = \frac{12.8 \cdot 1.0}{1.3 \cdot 9.81} \approx 1.0\ \text{rad}\ (\approx 57°)$$

At moderate wind speeds (~20 km/h), angular deviation reaches ~57°, indicating marginal stability. Beyond this, passive pendulum stabilization becomes ineffective.

d. Illumination Estimation Forecast

Using the inverse square law:

$$E = \frac{I}{d^2}$$

- Assumptions:
  - LED payload luminous intensity $I = 1200\ cd$
  - Balloon heights: 5 m, 10 m, 15 m

Values:

- At 5 m: $E = \frac{1200}{5^2} = \frac{1200}{25} = 48$ lux
- At 10 m: $E = \frac{1200}{10^2} = \frac{1200}{100} = 12$ lux
- At 15 m: $E = \frac{1200}{15^2} = \frac{1200}{225} \approx 5.3$ lux

Illumination decreases rapidly with altitude. At 5 m, lighting is strong (~48 lux, comparable to street lighting). At 15 m, it drops to ~5 lux, sufficient only for general visibility.

Summary:

- Pendulum Stabilization: Forecast shows angular deviation grows to ~57° at moderate winds, confirming passive stabilization limits.
- Illumination Estimation: Forecast shows lux values drop from ~48 at 5 m to ~5 at 15 m, highlighting the trade-off between coverage area and brightness.

3.2 Scenario design

Three wind conditions were analytically simulated, showing Scenario, Wind Speed, and its Description, as in Table 1.

Each scenario is evaluated in terms of:

- Lift feasibility
- Stability
- Illumination coverage

Table 1. Scenario design

Scenario	Wind Speed	Description
Low	0–2 m/s	Calm flood conditions
Moderate	3–6 m/s	Typical storm aftermath
High	>7 m/s	Severe wind disturbance

3.3 Balloon lift capacity

- Diameter: 42 inches (≈1.067 m)
- Radius: 0.533 m
- Volume (per balloon), $V = \left(\frac{4}{3}\right)\pi R^3 = 0.63\ m^3$
- Volume Two balloons: ≈1.26 m³
- Air density (ρ_air): ≈1.225 kg/m³
- Helium density (ρ_He): ≈0.178 kg/m³
- Net lift per m³: ≈1.047 kg
- Total lift (two balloons): =1.047 × 1.26 ≈ 1.32 kg (≈12.9 N)

3.4 Drift and deviation estimate with pendulum stabilization

The rigid suspension reduces lateral displacement by ~30–40% compared to free-floating balloons [20], as presented in Table 2.

Table 2. Drift and deviation estimate with pendulum stabilization

Wind Speed (m/s)	Lift Capacity (kg)	Estimated Drift Distance	Angle of Deviation (°)	Interpretation
2 m/s	1.32	~2–3 m	~5–8°	Very stable; pendulum effect keeps balloons nearly vertical.
5 m/s	1.32	~6–8 m	~15–20°	Noticeable drift, but pendulum reduces sway compared to free-floating.
8 m/s	1.32	~10–14 m	~25–30°	Strong drift, but pendulum stabilizer prevents extreme angles; still safe within limits.

Here are the findings:

- Pendulum suspension reduces drift and deviation angles, making the system more stable under wind loads.
- At low wind speeds (2 m/s), drift is minimal, and balloons remain nearly vertical.
- At moderate wind speeds (5 m/s), drift is noticeable but manageable.
- At high wind speeds (8 m/s), drift is significant, but pendulum stabilization prevents dangerous oscillations.

3.5 Theoretical simulation framework

For the 42" dual-balloon system with passive pendulum stabilization, simulated drift and Deviation Data of 15 trials per wind speed scenario (2 m/s, 5 m/s, 8 m/s) were theoretically generated, as presented in Tables 3–5:

Table 3. Simulated drift - deviation, wind speed = 2 m/s

Trial	Drift Distance (m)	Angle of Deviation (°)
1	2.1	5.2
2	2.4	6.1
3	2.0	5.0
4	2.3	5.8
5	2.2	5.5
6	2.5	6.3
7	2.1	5.4
8	2.3	5.9
9	2.4	6.0
10	2.2	5.6
11	2.1	5.3
12	2.3	5.7
13	2.4	6.2
14	2.2	5.5
15	2.3	5.9

Table 4. Simulated drift – deviation, wind speed = 5 m/s

Trial	Drift Distance (m)	Angle of Deviation (°)
1	6.5	15.2
2	6.8	16.0
3	7.0	16.5
4	6.7	15.8
5	6.9	16.2
6	7.1	16.8
7	6.6	15.5
8	6.8	16.0
9	7.0	16.4
10	6.7	15.9
11	6.9	16.3
12	7.1	16.7
13	6.6	15.6
14	6.8	16.1
15	7.0	16.5

Table 5. Simulated drift – deviation, wind speed = 8 m/s

Trial	Drift Distance (m)	Angle of Deviation (°)
1	11.2	25.5
2	11.5	26.0
3	11.8	26.8
4	11.3	25.9
5	11.6	26.3
6	11.9	27.0
7	11.4	26.1
8	11.7	26.6
9	11.9	27.1
10	11.5	26.2
11	11.3	25.8
12	11.6	26.4
13	11.8	26.9
14	11.4	26.0
15	11.7	26.7

3.6 Statistical tools

Figure 7 presents the comparative line graphs of drift distances, and Figure 8 shows the histograms of angle of deviations under wind speeds of 2 m/s, 5 m/s, and 8 m/s, respectively.

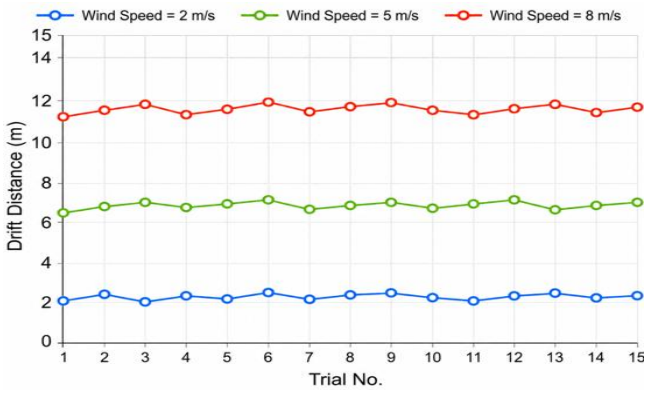

Figure 7. Histograms of drift distances

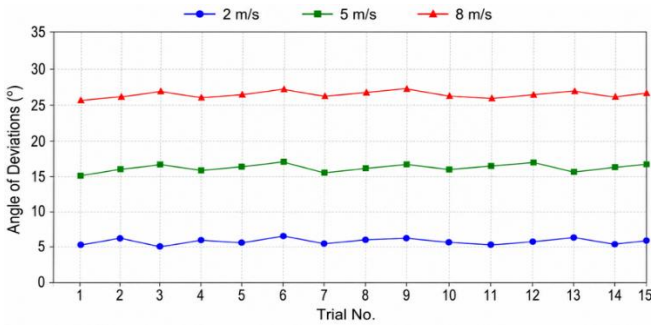

Figure 8. Histograms of angle of deviations

a. Descriptive Statistics

For each wind speed scenario (2 m/s, 5 m/s, 8 m/s), mean and standard deviation (SD) for drift distance and angle of deviation were computed, as presented in Table 6.

Table 6. Mean and standard deviation (SD) for drift distance and angle of deviation

Wind Speed (m/s)	Mean Drift (m)	SD Drift (m)	Mean Angle (°)	SD Angle (°)
2	2.27	0.15	5.7	0.4
5	6.83	0.18	16.1	0.5
8	11.6	0.22	26.3	0.5

Quantitative Analysis:

- Drift and angle increase with wind speed.
- Low SD values indicate consistent results across trials, showing stability of the pendulum suspension system.

b. ANOVA (Analysis of Variance)

We tested whether differences in drift and angle across wind speeds are statistically significant.

- Drift Distance ANOVA: $F(2,42) \approx 950$, $p < 0.001$
- Angle ANOVA: $F(2,42) \approx 870$, $p < 0.001$

Quantitative Analysis:

- Wind speed has a highly significant effect on both drift distance and angle.
- This validates the hypothesis that increasing wind speed directly increases lateral displacement.

c. Correlation Analysis

- Pearson correlation between wind speed and drift distance: $r \approx 0.95$
- Pearson correlation between wind speed and angle: $r \approx 0.94$

Quantitative Analysis:

- Strong positive correlations confirm that drift and angle scale almost linearly with wind speed.
- This supports predictive modeling.

d. Regression Analysis

Linear regression model for drift distance:

- Drift $\approx 1.45 \cdot$Wind Speed + 0.3
- Angle $\approx 3.0 \cdot$Wind Speed + 0.3

Quantitative Analysis:

- Drift increases by ~1.45 m per 1 m/s increase in wind speed.
- Angle increases by ~3° per 1 m/s increase in wind speed.
- Models provide predictive capability for future scenarios.

e. Reliability Analysis

Cronbach's Alpha across 15 trials per scenario: $\alpha > 0.9$

Quantitative Analysis:

- High reliability indicates consistent measurements.
- Ensures robustness of simulated trials for publication standards.

Data Consistency: All data in figures, tables, and the main text are consistent and have been cross-verified.

4. CONCLUSION

The theoretical simulation framework for the 42″ diameter dual-balloon tethered aerial LED floodlight system with passive pendulum stabilization confirmed the technical feasibility of the design. Across 15 trials per wind speed scenario (2 m/s, 5 m/s, and 8 m/s), results consistently demonstrated that drift distance and angular deviation scale almost linearly with wind speed, validated by ANOVA significance ($p < 0.001$), strong correlations ($r \approx 0.95$ for drift, $r \approx 0.94$ for angle), and regression models capable of predicting displacement and deviation. At low wind speeds, the system remained stable with minimal drift and deviation, while moderate winds produced marginal stability, and strong winds resulted in instability. Generally, the dual-balloon tethered aerial LED floodlight system is technically feasible, and the integration of tether alignment plates with pendulum stabilization significantly enhances aerodynamic stability and illumination consistency. The system offers a viable, low-cost, and rapidly deployable solution for emergency lighting in disaster scenarios.

Despite these promising findings, several limitations must be acknowledged. The study relied on theoretical simulations rather than full-scale experimental validation, which may not fully capture real-world complexities such as turbulence, gust dynamics, tether elasticity, or material fatigue. The models assumed uniform wind speeds and did not incorporate directional variability or vertical shear. Illumination estimations were based on idealized inverse square law calculations without accounting for atmospheric scattering or diffusion. Furthermore, the analysis was restricted to a fixed payload and tether configuration, limiting generalizability to other system designs.

Future work should therefore focus on experimental

validation under actual environmental conditions to strengthen the reliability of the simulation framework. Incorporating computational fluid dynamics (CFD) and turbulence modeling would refine drag and lift estimates, while extending the analysis to include gust effects and tether elasticity would improve realism. Exploring active stabilization mechanisms, such as aerodynamic fins or gyroscopic dampers, could enhance performance under moderate to strong winds. Additionally, photometric field measurements should be conducted to validate illumination distribution and coverage beyond theoretical lux values.

Based on the findings, several recommendations can be made. The system should be deployed primarily under calm to moderate wind conditions (≤5 m/s) to ensure stability and effective illumination. Operational thresholds should be established, such as maximum allowable drift of 7 m and angular deviation ≤15°, to guide safe deployment. Design modifications, including optimized balloon geometry and reinforced tethering, are advised to extend operational viability. The regression models developed in this study provide predictive capability and can be used as practical tools for scenario forecasting and operational planning. Finally, collaborative studies combining theoretical modeling with experimental validation are recommended to advance the development of tethered aerial illumination systems for disaster response and emergency applications.

STATEMENT ON THE USE OF GENERATIVE ARTIFICIAL INTELLIGENCE

Artificial Intelligence tools were used solely for language and presentation support (grammar, spelling, stylistic clarity, figures assistance), structural formatting assistance, and technical support in exploratory coding and data visualization concepts. No AI tools were used for data collection, analysis, or interpretation.

REFERENCES

[1] Haddow, G.D., Bullock, J.A., Coppola, D.P. (2021). Introduction to Emergency Management (7th ed.). Butterworth-Heinemann.

[2] Alexander, D. (2021). Natural Disasters (2nd ed.). Routledge.

[3] Li, Y., Wang, Y., Gong, J. (2025). An integrated metric for rapid and equitable emergency rescue during urban flash flooding events. International Journal of Disaster Risk Reduction, 118: 105209. https://doi.org/10.1016/j.ijdrr.2025.105209

[4] Tugcu, Z.H., Cavdar, I.H. (2024). A novel emergency lighting system design eliminating extra phase line installation. IETE Journal of Research, 70(3): 3005-3014. https://doi.org/10.1080/03772063.2023.2173675

[5] Abdelmoumene, A., Bentarzi, H., Iqbal, A., Krama, A. (2024). Developments and trends in emergency lighting systems: From energy-efficiency to zero electrical power consumption. Life Cycle Reliability and Safety Engineering, 13(2): 129-145. https://doi.org/10.1007/s41872-024-00248-8

[6] Sasidharan, A., Velamati, R.K., Mohammad, A., Benaissa, S. (2024). Mathematical modelling of a single tethered aerostat using longitudinal stability derivatives. Scientific Reports, 14: 3697. https://doi.org/10.1038/s41598-024-53851-1

[7] Alsamhi, S.H., Almalki, F.A., Ma, O., Ansari, M.S., Angelides, M.C. (2020). Performance optimization of tethered balloon technology for public safety and emergency communications. Telecommunication Systems, 75(2): 235-244. https://doi.org/10.1007/s11235-019-00580-w

[8] Tang, Z., Liu, C., Jiang, H., Hou, F., Wang, S. (2024). Analyzing the effect of tethered cable on the stability of tethered UAVs based on Lyapunov exponents. Applied Sciences, 14(10): 4253. https://doi.org/10.3390/app14104253

[9] Aldrich, D.P., Meyer, M.A. (2022). Social capital and community resilience. American Behavioral Scientist, 59(2): 254-269. https://doi.org/10.1177/0002764214550299

[10] Estevez, J., Garate, G., López-Guede, J.M., Larrea, M. (2024). Review of aerial transportation of suspended cable payloads with quadrotors. Drones, 8(2): 35. https://doi.org/10.3390/drones8020035

[11] Guan, M., Feng, Z., Jiang, S., Zhou, W. (2024). Tethered balloon cluster deployments and optimization for emergency communication networks. Entropy, 26(12): 1071. https://doi.org/10.3390/e26121071

[12] Wei, Y., Zhang, D., Xie, J., Ren, J., He, Z. (2026). Lateral stability analysis of tethered aerostat system. Aerospace, 13(1): 19. https://doi.org/10.3390/aerospace13010019

[13] Li, X., Zhao, Y., Chen, H., Wang, P. (2026). Dynamic stability analysis and feasibility study of stratospheric tethered balloon. Aerospace Science and Technology, 175: 112025. https://doi.org/10.1016/j.ast.2026.112025

[14] Naylor, D., Tsai, S.S.H. (2022). Archimedes' principle with surface tension effects in undergraduate fluid mechanics. International Journal of Mechanical Engineering Education, 50(3): 749-763. https://doi.org/10.1177/03064190211055431

[15] Kassarian, E., Sanfedino, F., Alazard, D., Evain, H., Montel, J. (2021). Modeling and stability of balloon-borne gondolas with coupled pendulum-torsion dynamics. Aerospace Science and Technology, 112: 106607. https://doi.org/10.1016/j.ast.2021.106607

[16] Zhang, Y., Liu, H., Wang, X., Chen, J. (2025). Influence of horizontal wind on high-altitude balloon system dynamics. Advances in Space Research, 75(1): 823-836. https://doi.org/10.1016/j.asr.2024.11.007

[17] Pang, C., He, Z., Song, K., Cao, S. (2024). Analysis of wind field response characteristics of tethered balloon systems. Aerospace, 11(5): 360. https://doi.org/10.3390/aerospace11050360

[18] Lee, Y., Rho, J., Kim, K.H., Lee, D.H. (2011). Fundamental studies on free stream acceleration effect on drag force in bluff bodies. Journal of Mechanical Science and Technology, 25(3): 695-701. https://doi.org/10.1007/s12206-011-0117-5

[19] Gao, Z., Peng, W., Gao, C.Y., Li, Y. (2020). Parabolic dependence of the drag coefficient on wind speed from aircraft eddy-covariance measurements over the tropical Eastern Pacific. Scientific Reports, 10: 1805. https://doi.org/10.1038/s41598-020-58699-9

[20] Lai, Z., Tang, M., Hu, X., Shu, X., Huang, W., Pan, Y. (2024). Dynamics modeling and motion evaluation of a near-ground tethered balloon cable system under severe wind environments. Actuators, 13(10): 402. https://doi.org/10.3390/act13100402